

Clinical Results of Immune Therapy and Radiation

# Impact of Sequencing Radiation Therapy and Immune Checkpoint Inhibitors in the Treatment of Melanoma Brain Metastases



Daniel A. Pomeranz Krummel, PhD,<sup>\*,1</sup> Tahseen H. Nasti, PhD,<sup>†,1</sup>  
Benjamin Izar, MD, PhD,<sup>‡,2</sup> Robert H. Press, MD,<sup>§,2</sup> Maxwell Xu, BS,<sup>\*,2</sup>  
Lindsey Lowder, DO,<sup>||</sup> Laura Kallay, PhD,<sup>\*</sup> Manali Rupji, MS,<sup>¶</sup>  
Havi Rosen, BSc,<sup>\*</sup> Jing Su, PhD,<sup>#</sup> Walter Curran, MD,<sup>§,¶</sup>  
Jeffrey Olson, MD,<sup>¶,\*\*</sup> Brent Weinberg, MD,<sup>††</sup>  
Matthew Schniederjan, MD,<sup>||</sup> Stewart Neill, MD,<sup>||</sup> David Lawson, MD,<sup>¶,††</sup>  
Jeanne Kowalski, PhD,<sup>§§</sup> Mohammad K. Khan, MD, PhD,<sup>§,¶</sup>  
and Soma Sengupta, MD, PhD<sup>\*,|||</sup>

<sup>\*</sup>Department of Neurology, University of Cincinnati College of Medicine, Cincinnati, Ohio;

<sup>†</sup>Department of Microbiology and Immunology, Emory University, Atlanta, Georgia; <sup>‡</sup>Columbia Center for Translational Immunology, Columbia University Medical Center, New York City, New York;

<sup>§</sup>Department of Radiation Oncology, Emory University School of Medicine, Atlanta, Georgia;

<sup>||</sup>Department of Pathology and Laboratory Medicine, Emory University School of Medicine, Atlanta, Georgia; <sup>¶</sup>Winship Cancer Institute, Emory University School of Medicine, Atlanta, Georgia;

<sup>#</sup>Department of Biostatistics and Data Science, Wake Forest School of Medicine, Winston-Salem, North Carolina; <sup>\*\*</sup>Department of Neurosurgery, Emory University School of Medicine, Atlanta, Georgia; <sup>††</sup>Department of Radiology and Imaging Sciences, Emory University School of Medicine, Atlanta, Georgia; <sup>††</sup>Department of Hematology and Medical Oncology, Emory University School of

Corresponding author. Mohammad K. Khan, MD, PhD and Soma Sengupta, MD, PhD; E-mail: [drkhurram2000@gmail.com](mailto:drkhurram2000@gmail.com) or [soma.sengupta@uc.edu](mailto:soma.sengupta@uc.edu)

Disclosure: J.O. reports editorial consultancy for American Cancer Society. M.K.K. reports a grant from Merck Pharmaceuticals, outside the submitted work. S.S. reports advisory role for Novocure.

Authors responsible for statistical analysis: Statistical analysis of patient data was conducted by co-authors Manali Rupji and Jeanne Kowalski.

Data availability: Sequence data generated in this study has been deposited in GEO Bank (accession number GSE131521). The source data underlying Figs. 1a, 1b, 2, 3b, and Supplementary Fig. 1 are provided as a source data file. The source data file has been deposited in the Open Science Framework (OSF) repository ([https://osf.io/5uwz7/?view\\_only=f3a998f613e543288d342d245569b81e](https://osf.io/5uwz7/?view_only=f3a998f613e543288d342d245569b81e)). The authors declare that all other data supporting the findings of this study are available within the main article and its Supplementary Information file or from corresponding authors upon reasonable request.

Financial support for the project came from: NIH-NINDS under award number NS083626 to S.S. (to support salary); Winship Cancer Institute

Melanoma Philanthropic Funds to S.S. and M.K.K.; American Cancer Society Institutional Research Grant to M.K.K.; Department of Radiation Oncology, Emory University Research Funds to M.K.K.; Merck Sharp & Dohme Corp. to M.K.K.; NIH-NCI K08-CA222663 and NIH U54-CA225088 to B.I.; the SITC-BMS Cancer Immunotherapy Translational Fellowship to B.I.; a Burroughs Wellcome Fund Career Award for Medical Scientists to B.I.; the Ludwig Center for Cancer Research at Harvard to B.I.; Department of Oncology, LIVESTRONG Cancer Institutes, Dell Medical School, University of Texas at Austin, TX, Research Funds to J.K. Research reported in this publication was also supported in part by the Biostatistics & Bioinformatics and the Integrated Cellular Imaging Shared Resources of the Winship Cancer Institute of Emory University and National Institutes of Health/National Cancer Institute under award number P30CA138292. The content is solely the responsibility of the authors and does not necessarily represent the official views of the National Institutes of Health.

Supplementary material for this article can be found at <https://doi.org/10.1016/j.ijrobp.2020.01.043>

<sup>1</sup> Co-first authors.

<sup>2</sup> Co-second authors.

Medicine, Atlanta, Georgia; <sup>§§</sup>Department of Oncology, LIVESTRONG Cancer Institutes, Dell Medical School, University of Texas, Austin, Texas; and <sup>|||</sup>University of Cincinnati Gardner Neuroscience Institute, Cincinnati, Ohio.

Received Aug 8, 2019, and in revised form Jan 15, 2020. Accepted for publication Jan 25, 2020.

### Summary

Melanoma brain metastases occur in ~50% of melanoma patients. Our study provides initial insights into the optimal sequence of radiation and immune checkpoint inhibitor in the treatment of melanoma brain metastases following surgical resection. Based on our analysis, a clinical trial examining the optimal sequence of radiation and immune checkpoint inhibitor is warranted.

**Purpose:** Melanoma brain metastases (MBM) occur in ~50% of melanoma patients. Although both radiation therapy (RT) and immune checkpoint inhibitor (ICI) are used alone or in combination for MBM treatment, the role of this combination and how these treatments could best be sequenced remains unclear.

**Methods and Materials:** We conducted a retrospective analysis of patients with resected MBM who underwent treatment with RT, ICI, or a combination of RT and ICI. Among the latter, we specifically investigated the differential gene expression via RNA-sequencing between patients who received RT first then ICI (RT → ICI) versus ICI first then RT (ICI → RT). We used a glycoprotein-transduced syngeneic melanoma mouse model for validation experiments.

**Results:** We found that for patients with resected MBM, a combination of RT and ICI confers superior survival compared with RT alone. Specifically, we found that RT → ICI was superior compared with ICI → RT. Transcriptome analysis of resected MBM revealed that the RT → ICI cohort demonstrated deregulation of genes involved in apoptotic signaling and key modulators of inflammation that are most implicated in nuclear factor kappa-light-chain-enhancer of activated B cells signaling. In a preclinical model, we showed that RT followed by anti-programmed death-ligand 1 therapy was superior to the reverse sequence of therapy, supporting the observations we made in patients with MBM.

**Conclusions:** Our study provides initial insights into the optimal sequence of RT and ICI in the treatment of MBM after surgical resection. Prospective studies examining the best sequence of RT and ICI are necessary, and our study contributes to the rationale to pursue these. © 2020 The Authors. Published by Elsevier Inc. This is an open access article under the CC BY-NC-ND license (<http://creativecommons.org/licenses/by-nc-nd/4.0/>).

## Introduction

Brain metastases are the most common intracranial malignancy in adult cancer patients. Melanoma accounts for ~10% of brain metastases, and ~50% of melanoma patients with advanced disease develop clinically overt melanoma brain metastasis (MBM). Recently, it has been shown that immune checkpoint inhibitors (ICIs) produce intracranial response rates comparable to those previously described for extracranial systemic responses.<sup>1-4</sup> Notably, analysis of the MBM study was restricted to asymptomatic patients who did not require radiation therapy (RT), neurosurgery, or steroids at time of enrollment. There is increasing preclinical and clinical rationale for synergistic effects of combining RT with ICI<sup>5-7</sup>; however, radiation dose, fraction size, and temporal sequence with ICI (before, concurrent, or after RT) remain unclear.<sup>8-10</sup>

## Methods and Materials

### Patient data

We conducted a retrospective analysis of patients from our institutional pathology database from 2010 to 2018 who had

resection of a single MBM and received central nervous system directed RT (n = 8) or ICI and RT (n = 17) (Table 1). For patients with eligible samples, relevant clinical information was captured from the electronic medical record under an institutional review board (IRB)-approved protocol (IRB00072396: "RAD2620-13: Melanoma Outcomes in Patients Receiving Radiation Therapy"). Patient characteristics captured included age at the time of brain resection, gender, presence of active systemic disease (defined as newly diagnosed metastatic disease and/or systemic progression within the last 3 months), presence of active extracranial metastases, Eastern Cooperative Oncology Group performance status, total number of brain metastases (including intact lesions), and melanoma molecular graded prognostic assessment score. Most patients received adjuvant RT after resection of the MBM (n = 11) compared with resection for local progression after initial RT (n = 6). Treatment characteristics included timing and use of systemic therapies (BRAF inhibitor and immunotherapy), extent of surgical resection (gross total or subtotal resection), and type of brain radiation (whole-brain radiation therapy [WBRT], stereotactic radiosurgery [SRS], or none). Type of radiation treatment was determined by the treating physician based on number of brain metastases per institutional practice. Both linear accelerator-based SRS

and Leskell Gamma Knife (Elekta AB, Stockholm, Sweden) SRS were used based on the treating facility. The prescribed dose was determined per recommendations from Radiation Therapy Oncology Group 9005. WBRT was delivered using 3-dimensional conformal opposed lateral fields with multileaf collimation. The prescribed dose was determined per physician preference.

## Survival analysis

Kaplan-Meier curves were created using the CASAS tool. CASAS is a Graphic user interface (R package) tool based on survival for comparing groups<sup>11</sup> A log-rank test was used to test for significant differences in survival. Univariate associations were estimated using the Cox proportional hazards model, and hazard ratios with 95% confidence intervals are reported. The significance level was set to 0.1 given the small sample size of the cohort.

## RNA sequencing

Patient tissue was obtained at time of surgical resection under IRB-approved protocols. Tissue processing at time of surgery consisted of fixation in 10% neutral buffered formalin and routine overnight processing for permanent fixation and paraffin embedding (FFPE: formalin fixed paraffin embedded). A retrospective search within the institutional pathology database from 2010 to 2018 for “melanoma” (including search fields restricted to brain specimens) yielded 79 specimens. Cases that did not have a sufficient amount of tumor volume for sequencing and did not receive radiation or immunotherapy were excluded. Samples that yielded acceptable sequences for analysis were sent for sequencing at the Broad Institute Genomics Platform (Cambridge, MA). After exclusions, only 17 samples of the original 79 specimens met eligibility and had sufficient sequencing.

Tissues for light microscopy, immunohistochemistry, and DNA molecular analysis were sectioned from the FFPE blocks at 5 μm thickness. Sections were stained using hematoxylin (Richard-Allan Scientific 7211) and eosin-Y (Richard-Allan Scientific 7111) for microscopic examination. Histopathologic tumor classification was reviewed by 4 board certified (American Board of Pathology) neuropathologists. After histopathologic review, unstained sections were submitted for DNA analysis, specifically using the SNaPshot mutational panel primer extension-based method (Thermo-Fisher) and Cancer Mutation Panel 26 (Illumina) per hospital protocol (Table 1). Unstained slides (5 μm thick, nonheat-treated) from FFPE tissue blocks were sectioned, and areas of interest macrodissected by a board-certified neuropathologist using a corresponding hematoxylin and eosin-stained slide. RNA was extracted (Qiagen, AllPrep FFPE kit), quantified, and quality measured by the DV200 score (fraction of RNA fragments whose length is >200 nts). Samples not meeting minimum requirements (≥750 ng RNA, preferred concentration 10 ng/μL, DV200 > 0.3) were

**Table 1** Abbreviated\* melanoma brain metastasis patient data

Variable	Level	n (%) = 17	
<b>Patient characteristics</b>			
Age (years)	Median (range)	54 (34-81)	
Sex	Male	13 (76.5)	
	Female	4 (23.5)	
Race	White	17	
Brain metastases at melanoma	Yes	6 (35.3)	
Diagnosis	No	11 (64.7)	
Active systemic disease	Yes	14 (82.4)	
	No	3 (17.6)	
Presence of extracranial disease	Yes	14 (82.4)	
	No	3 (17.6)	
Number of brain metastases	Median (range)	2 (1-6)	
Pretreatment LDH	Median (range)	202 (121-312)	
BRAF mutation status	Mutated	9 (52.9)	
	Wild-type	8 (47.1)	
Melanoma molGPA	1-1.5	3 (17.6)	
	2.0-2.5	9 (52.9)	
	3.0-3.5	4 (23.5)	
	4.0	1 (5.9)	
<b>Treatment Characteristics</b>			
BRAF inhibitor use	Yes	5 (29.4)	
	No	12 (70.6)	
Immunotherapy timing	After RT (RT → ICI)	11 (64.7)	
	Before and after RT (ICI → RT)		6 (35.3)
Type of RT	SRS	15 (88.2)	
	WBRT	2 (11.8)	
RT Dose	SRS (dose/fractions)	Median (range)	21 (16-32.5)/1 (1-5)
	WBRT	Median (range)	33.75 (30-37.5) /12.5 (10-15)

*Abbreviations:* ICI = immune checkpoint inhibitor; LDH = lactate dehydrogenase; molGPA = molecular graded prognostic assessment; RT = radiation therapy; SRS = stereotactic radiosurgery; WBRT = whole-brain radiation therapy.

\* See source file deposited in the Open Science Framework (OSF) repository for detailed version of patient data (see Data availability).

held for further evaluation. Samples were processed and sequenced by Transcriptome Capture (Illumina HiSeq2500) at the Broad Institute.

## Gene expression analysis

Short-read sequences were aligned to the hg19 human reference genome using STAR (v2.4.1a). On average, we

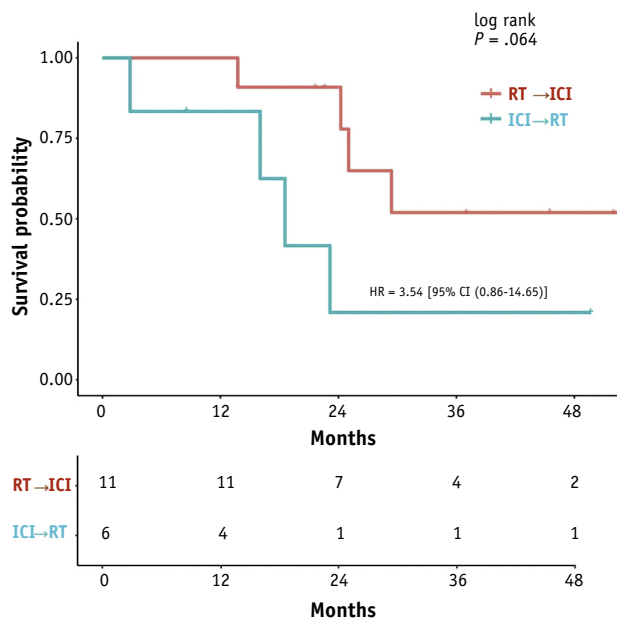


**Fig. 1.** Effect of timing. Kaplan-Meier curve of patients with melanoma brain metastases (MBM) who received radiation therapy (RT) and immunotherapy (n = 17) stratified according to immunotherapy timing: immunotherapy before and after RT (immune checkpoint inhibitors [ICI] → RT [cyan line, n = 6]) versus after RT (RT → ICI) (red line, n = 11) (Table 1). Hazard ratios (HR) based on Cox proportionality hazard models are reported for ICI → RT versus RT → ICI group (3.54 [0.86-14.65]), type 3  $P = .0808$ , log rank  $P = .064$ .

obtained 37,476,289 reads per brain metastasis sample. Feature counting with mapped bam files was used to obtain raw count files. SAMseq (<https://www.rdocumentation.org/packages/samr/versions/3.0/topics/SAMseq>) was used to conduct differential expression analysis, as it accounts for potential correlation in expression among genes and its permutation-based testing method was deemed more appropriate for a smaller sample size. After identifying differentially expressed genes (false discovery rate cutoff, 0.05), expression levels were normalized with samrR before being log<sub>2</sub> transformed.

## Mouse experiments

B16F10 cell line and Lentiviral vector expressing lymphocytic choriomeningitis glycoprotein (GP) were transduced per manufacturer instructions (Clontech). B16F10-GP cells ( $5 \times 10^5$ ) were implanted in matrigel on right and left flank of 6- to 8-week-old female C57BL/6 mice (Jackson Laboratories) in accordance with Institutional Animal Care and Use Committee guidelines. After tumors were palpable (10 days), mice were irradiated on the right side with a Superflab bolus (0.5 cm tissue equivalent material) placed over the tumor, and thereafter tumor measurements taken. An X-RAD 320 irradiation unit used a light beam ( $<8 \text{ mm}^2$ ) focused on the

tumor with mice under anesthesia. Tumor diameters were measured using calipers. Tumor volume was calculated using the formula for an ellipse (ie,  $4/3\pi \cdot [l \cdot w \cdot h]$ , where l, w, h are 3 radii of the tumor taken perpendicular to each other).

## Results

### Immunotherapy and radiation timing

Patients with MBM who received ICI and RT had superior survival compared with patients receiving RT alone (Fig. E1, available online at <https://doi.org/10.1016/j.ijrobp.2020.01.043>). We stratified those patients who received ICI and RT into 2 treatment groups: (1) RT followed by ICI (RT → ICI) (n = 11); and (2) ICI followed by RT and then ICI again (ICI → RT) (n = 6), where RT was either SRS (n = 15) or WBRT (n = 2). The median dose/fraction of SRS was 21 Gy/1 fraction (range, 16-32.5 Gy in 1-5 fractions). WBRT was delivered in 30 Gy/10 fractions and 37.5 Gy/15 fractions, respectively. Survival analysis suggests that the RT → ICI treatment group had an improved outcome (log-rank  $P = .064$ ) (Fig. 1). At 15 months, we observed a separation in curves for the “timing” analysis (Fig. 1), although the small sample size precludes our further testing the significance of this result.

### Differential gene expression analysis

To gain insights into the potential benefits of sequencing RT → ICI versus ICI → RT, we performed RNA-seq of the 17 included patients who received combination therapy of RT and ICI. Differential gene expression analysis of resected MBM between RT → ICI and ICI → RT treatment groups showed 48 deregulated genes (false discovery rate cut-off, 0.05), all increased in expression in the RT → ICI group (Fig. 2). Annotation/pathway enrichment analysis revealed a significant ( $P < .01$ , Table E1, available online at <https://doi.org/10.1016/j.ijrobp.2020.01.043>) enrichment of genes functionally involved in apoptosis and antiapoptotic signaling, including NIK (MAP3K14), key modulator of noncanonical nuclear factor kappa-light-chain-enhancer of activated B cells (NFKB) signaling; RIPK1, a receptor interacting kinase that also participates in NFKB as well as JNK and Akt signaling; and DAB2, previously reported as downregulated in ovarian cancer and has a role in immune regulation.

### Sequential administration of $\alpha$ -programmed death-ligand 1 and radiation in vivo

We next aimed to model the different sequences of RT/ICI combination therapy. We analyzed the clinical observation of improved outcome for RT → ICI (for ICI, we used an anti-programmed death-ligand 1 antibody) using the B16F10-GP syngeneic melanoma model (Fig. 3a). The

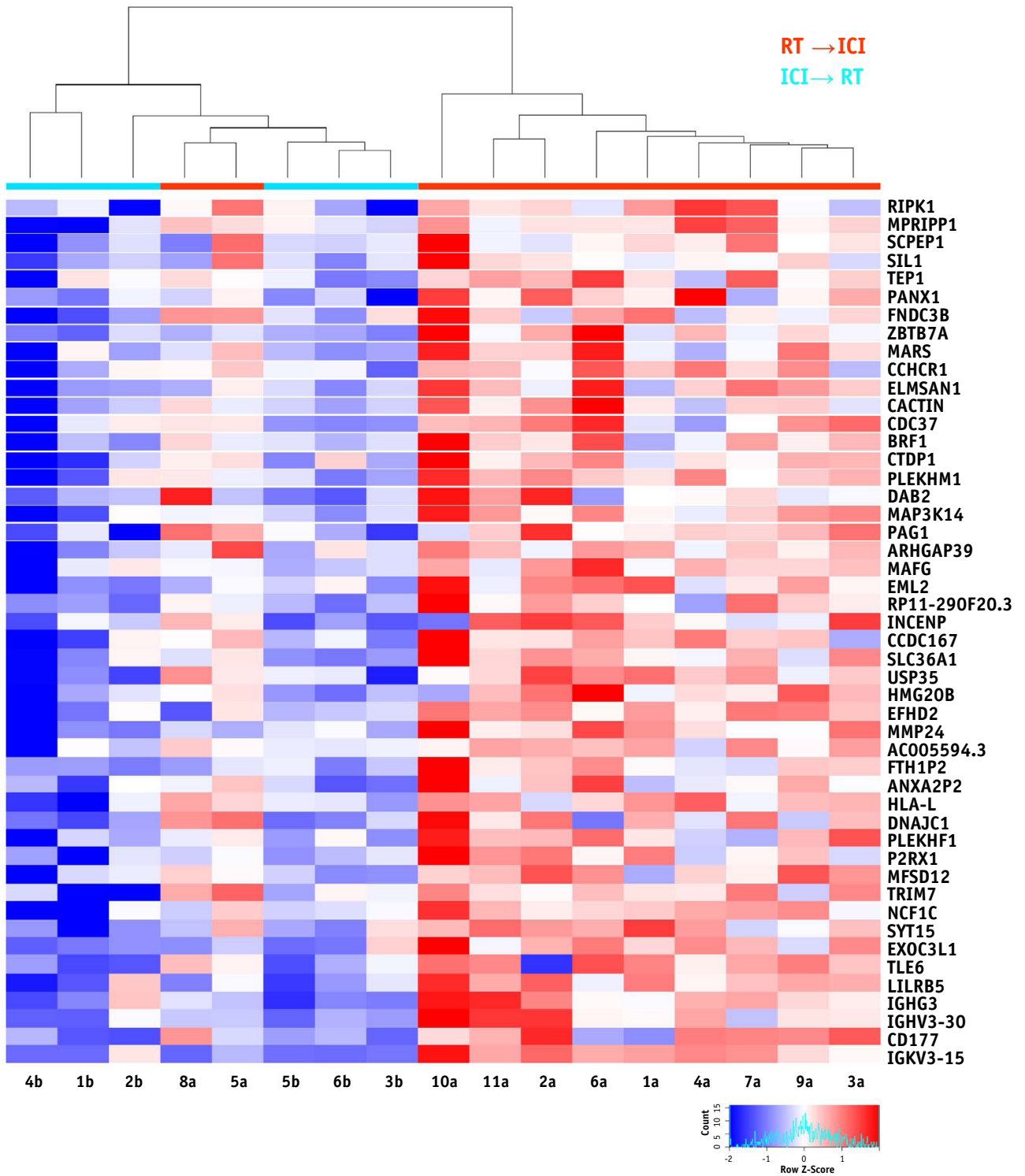


**Fig. 2.** Differential gene expression analysis. Unsupervised heatmap of differentially expressed genes (DEGs) (FDR < 0.05) of patients (n = 17). DEGs all have identical q-values and are ordered based on decreasing fold change, so that RIPK1 has highest and IGKV3.15 lowest. All DEGs were overrepresented in the radiation therapy (RT) before immunotherapy (ICI) treatment group (RT → ICI) relative to the ICI before and after RT group (ICI → RT). Gene expression data are labeled by therapeutic regimen: ICI → RT (cyan line, n = 6) versus RT → ICI (red line, n = 11). Patient's gene expression followed unsupervised clustering based upon euclidean distance metrics and the complete linkage method. After unsupervised clustering, the dendrogram clustered the majority of patient treatment groups with each other. Each patient/column has been assigned a number and letter, shown at the bottom of the heatmap, to aid identification of the patient in clinical Table 1. Abbreviation: FDR = false discovery rate.

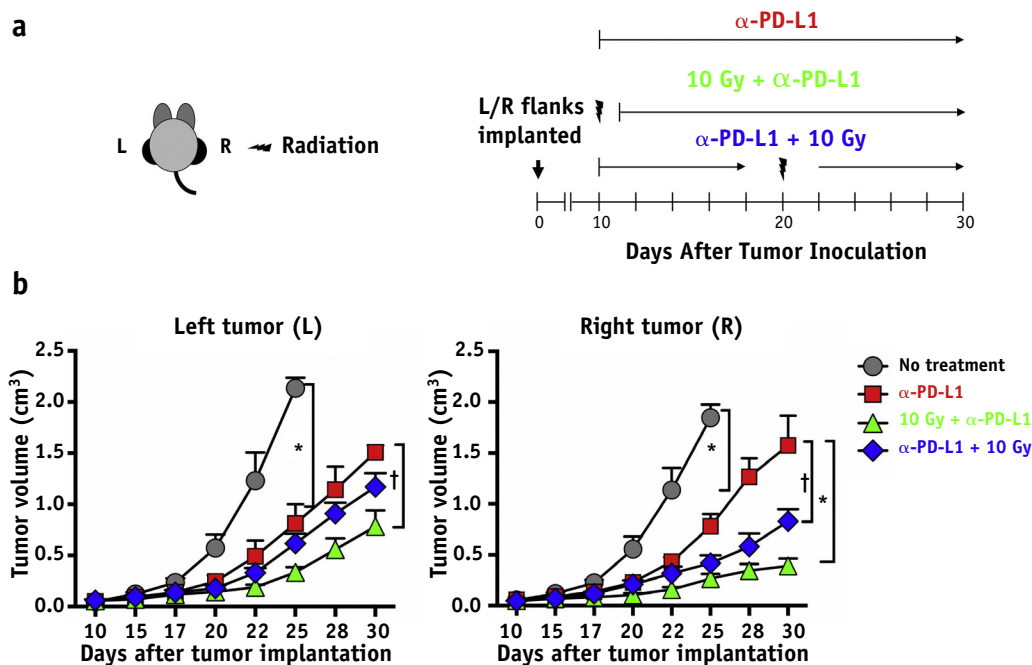


**Fig. 3.** Radiation and  $\alpha$ -PD-L1 response in vivo. (a) Mice implanted in left (L) and right (R) flanks with B16F10-GP cells received: (i) no treatment; (ii)  $\alpha$ -PD-L1 alone; (iii) 10 Gy (right flank) on day 10 (morning) before  $\alpha$ -PD-L1 (RT  $\rightarrow$  ICI) (evening); (iv)  $\alpha$ -PD-L1 first, followed by 10 Gy (right flank) on day 20 (ICI  $\rightarrow$  RT). Sequence of  $\alpha$ -PD-L1 and radiation is shown ( $n = 5$ ).  $\alpha$ -PD-L1 antibody (200  $\mu$ g; clone 29F.1A12) was in phosphate buffered saline (500  $\mu$ L). (b) Mean tumor volumes of right and left tumors after different treatments ( $*P < .01$ ,  $^{\dagger}P < .05$ ). Tumor measurements were taken with at least 5 mice per group ( $*P < .01$ ,  $^{\dagger}P < .05$ ). Using analysis of variance (ANOVA) followed by Tukey, the 2 treatment groups had a  $P$  value of .05 for the right side, and on the left side they were not significantly different. Difference between the 2 treatment groups by  $t$  test: the 2 groups were significantly different from one another on the right side ( $P < .001$ ), and the left side  $P$  value was .055. *Abbreviation:* PD-L1 = programmed death-ligand 1.

best tumor control within the irradiated volume and nonirradiated region (the “abscopal site”) was noted for RT  $\rightarrow$  ICI (Fig. 3b), consistent with the observation that patients who received RT  $\rightarrow$  ICI had improved outcomes (Fig. 1b). No antitumor activity was observed when CD8 T cells were depleted, indicating that T cells were necessary for responses to  $\alpha$ -programmed death-ligand 1 therapy in combination with RT (Fig. E2, available online at <https://doi.org/10.1016/j.ijrobp.2020.01.043>).

## Discussion

Our pilot study indicates that delivering RT followed by ICI may result in superior survival in MBM patients compared with RT or ICI alone, or ICI followed by RT. In line with our study, several smaller studies indicate an acceptable toxicity profile of RT plus ICI and potentially improved responses in patients with MBM.<sup>12-14</sup> Transcriptome analysis of resected MBM indicated changes in expression of a limited set of genes, and pathway analysis indicates involvement of the NF $\kappa$ B signaling pathway. In line with our observations, RT induces various mechanisms that may enhance response to subsequent therapy

with ICI, including enhanced antigen-presenting cells, induction of immune stimulatory cytokines and chemokines, enhanced T cell infiltration, induction of immune stimulatory cytokine production by T cells, maintenance of T cell effector function, and partial reversal of T cell dysfunction.<sup>15-17</sup> Of note, an important consideration when interpreting the RNA-seq data from this study is the timing of tumor resection and RT/ICI. The majority of evaluated specimens (11 of 17) were resected before adjuvant RT, suggesting that the differential gene expression may be more representative of intrinsic tumor biology than effects of prescribed therapies. However, the clinical outcomes still suggest sequential RT  $\rightarrow$  ICI therapy results in improved antitumor responses, and our murine model results support these clinical observations. A preclinical MBM model is needed to further functionally dissect the role of different sequencing strategies of RT and ICI.

In summary, our current study contributes to increasing evidence that sequencing RT and ICI may have differential effects on the outcomes of patients with MBM and prospective studies to validate this are reasonable and necessary. We aim to design a prospective clinical study with sufficient patient numbers that would enable us to

more fully explore this research and validate the results presented herein based on retrospective, small tissue samples.

## References

1. Tawbi HA, Forsyth P, Algazi A, et al. Combined nivolumab and ipilimumab in melanoma metastatic to the brain. *N Engl J Med* 2018; 379:722-730.
2. Postow MA, Sidlow R, Hellmann MD. Immune-related adverse events associated with immune checkpoint blockade. *N Engl J Med* 2018; 378:158-168.
3. Wolchok JD, Chiarion-Sileni V, Gonzalez R, et al. Overall survival with combined nivolumab and ipilimumab in advanced melanoma. *N Engl J Med* 2017;377:1345-1356.
4. Larkin J, Hodi FS, Wolchok JD. Combined nivolumab and ipilimumab or monotherapy in untreated melanoma. *N Engl J Med* 2015;373: 1270-1271.
5. Dewan MZ, Galloway AE, Kawashima N, et al. Fractionated but not single-dose radiotherapy induces an immune-mediated abscopal effect when combined with anti-CTLA-4 antibody. *Clin Cancer Res* 2009;15.
6. Antonia SJ, Villegas A, Daniel D, et al. Durvalumab after chemoradiotherapy in stage iii non-small-cell lung cancer. *N Engl J Med* 2017;377:1919-1929.
7. Marconi R, Strolin S, Bossi G, Strigari L. A meta-analysis of the abscopal effect in preclinical models: Is the biologically effective dose a relevant physical trigger? *PLoS One* 2017;12:e0171559.
8. Chowdhary M, Patel KR, Danish HH, Lawson DH, Khan MK. BRAF inhibitors and radiotherapy for melanoma brain metastases: potential advantages and disadvantages of combination therapy. *Onco Targets Ther* 2016;9:7149-7159.
9. Patel KR, Chowdhary M, Switchenko JM, et al. BRAF inhibitor and stereotactic radiosurgery is associated with an increased risk of radiation necrosis. *Melanoma Res* 2016;26:387-394.
10. Khan MK, Khan N, Almasan A, Macklis R. Future of radiation therapy for malignant melanoma in an era of newer, more effective biological agents. *Onco Targets Ther* 2011;4:137-148.
11. Rupji M, Zhang X, Kowalski J. CASAS: Cancer Survival Analysis Suite, a web based application. *F1000Research* 2017;6:919; 12.
12. Patel KR, Lawson DH, Kudchadkar RR, et al. Two heads better than one? Ipilimumab immunotherapy and radiation therapy for melanoma brain metastases. *Neuro Oncol* 2015;17:1312-1321.
13. Hiniker SM, Reddy SA, Maecker HT, et al. A prospective clinical trial combining radiation therapy with systemic immunotherapy in metastatic melanoma. *Int J Radiat Oncol Biol Phys* 2016;96:578-588.
14. Twyman-Saint VC. Radiation and dual checkpoint blockade activate non-redundant immune mechanisms in cancer. *Nature* 2015;520: 373-377.
15. Tang C, Welsh JW, de Groot P, et al. Ipilimumab with stereotactic ablative radiation therapy: phase i results and immunologic correlates from peripheral T cells. *Clin Cancer Res* 2017;23:1388-1396.
16. Buchwald ZS, Wynne J, Nasti TH, et al. Radiation, immune checkpoint blockade and the abscopal effect: A critical review on timing, dose and fractionation. *Front Oncol* 2018;8:612.
17. Lumniczky K, Safrany G. The impact of radiation therapy on the antitumor immunity: Local effects and systemic consequences. *Cancer Lett* 2015;356:114-125.